



An experimental test of semiclassical radiation theories
by John Milton Wessner

A thesis submitted to the Graduate Faculty in partial fulfillment of the requirements for the degree of
DOCTOR OF PHILOSOPHY in Physics
Montana State University
© Copyright by John Milton Wessner (1972)

Abstract:

An experiment is described which tests the semi-classical radiation theory proposed by E. T. Jaynes and his collaborators. Their work predicted that the $n = 2$ level of hydrogen will have a lifetime which varies linearly with the 2s state population for small excited state components. By applying a short electrical pulse to a 60 keV atomic hydrogen beam with a 2s population of approximately 9%, the variation of the lifetime could be measured as a function of the 2s occupation after the pulse. A total change of approximately + 4% is predicted while the observed change was -.2%.

AN EXPERIMENTAL TEST OF SEMICLASSICAL RADIATION THEORIES

by

JOHN MILTON WESSNER

A thesis submitted to the Graduate Faculty in partial
fulfillment of the requirements for the degree

of

DOCTOR OF PHILOSOPHY

in

Physics

Approved:

Robert J. Swenson
Head, Major Department

David K. Anderson
Chairman, Examining Committee

Henry L. Parsons
Graduate Dean

MONTANA STATE UNIVERSITY
Bozeman, Montana

August, 1972

PREFACE

Each of us is attracted to physics by some deep impression made upon him as a child. For me it was the atomic bomb, although the road from that point to now is so circuitous and disconnected that only my most antagonistically humanist friends can still detect the taint. A more tangible starting point is to be found in the reading of a little book by G. P. Thomson called The Inspiration of Science and finding that the richness found there could be shared with my students. Unfortunately, the joyous days of string and sealing wax were gone, as rockets went roaring into space from just up the road, and biologists traded in their microscopes for ultracentrifuges.

As a consequence, it is a distinct pleasure to present a piece of research here which seems to test a point with well delineated philosophical roots, using equipment which in some cases was not in existence ten years ago, and yet, in which the data have a rather clean interpretation. One likes to think that had the results

been the opposite that there would now be a run on string and sealing wax.

Because of the amount of historical nonsense I imbibed as a student and my own notion of the significance of this work, I have included in the first chapter a very sketchy history of quantum mechanics up to the enunciation of the principle of complementarity. Things which are common knowledge and true are often omitted, but the outline seemed appropriate in light of my background. The reader may skip to the last six paragraphs if he pleases.

It is customary to thank everyone in sight for their part in the production of a dissertation, and one does well at this point to adhere to custom. Thanks go to Alfred Romer for sending me to Montana and to B. Frank Brown in Melbourne for allowing me to become scholarly at long last. No thanks are due to those who held back; they have their own righteousness for comfort. My hungry children have benefitted from the generous support of the MSU physics department as well as everyone else from whom funds were mulcted.

I am grateful to professor D. K. Anderson for suggesting the original problem and retaining his sanity in the dark days when nothing seemed right, to professor R. T. Robiscoe for some very necessary capital equipment, and to Mr. C. F. Badgley for his advice and direct assistance in building the apparatus. Most of all, may eternal blessings shower upon my wife Sally who, after celebrating her thirtieth birthday at thirty below, three thousand miles from home, has remained steadfast to the revision of the fourth draft.

TABLE OF CONTENTS

Chapter	Page
I. Waves, Oscillators and Photons	1
II. Radiation Theory I:	
Quantum Electrodynamics	13
III. Radiation Theory II:	
Semiclassical Theory	22
IV. Apparatus	33
V. State preparation	67
VI. Results	82
VII. Uncertainties and Systematic Effects .	91
VIII. Conclusions	99
Appendices	
A. Metastable Quench in a Uniform Field .	102
B. Window Function	106
C. Quench Distributions	108
D. Electrode Field Measurements	110
E. Beam Averaging	119
F. Statistical Optimization	126
References	
Footnotes	131

LIST OF TABLES

Table	Page
I. Rate values	90

LIST OF FIGURES

Figure	Page
1. Three level atom	21
2. Schematic view of the apparatus	35
3. Experimental chamber interior	37
4. Exchange cell characteristics	41
5. Metastable fraction	43
6. Sweep destruction	46
7. Prequench electrode	49
8. Detector response	53
9. Light collection geometry	55
10. Electronic flow chart	58
11. CEM circuit	60
12. Beam detector	62
13. Collector characteristics	64
14. Electrodes	70
15. Quantum oscillations	72
16. Signal roll off	74
17. Predicted quantum oscillations	81
18. Exponential decay	86
19. Gaussian fits	113

Figure		Page
20.	Field inhomogeneity I	115
21.	Field inhomogeneity II	117
22.	Radiation intensity components I	123
23.	Radiation intensity components II	125

ABSTRACT

An experiment is described which tests the semi-classical radiation theory proposed by E. T. Jaynes and his collaborators. Their work predicted that the $n = 2$ level of hydrogen will have a lifetime which varies linearly with the $2s$ state population for small excited state components. By applying a short electrical pulse to a 60 keV atomic hydrogen beam with a $2s$ population of approximately 9%, the variation of the lifetime could be measured as a function of the $2s$ occupation after the pulse. A total change of approximately +4% is predicted while the observed change was -.2%.

CHAPTER I
WAVES, OSCILLATORS AND PHOTONS

The experiment described in this report is part of a continuing refinement of our understanding of the interaction of matter and electromagnetic radiation. It would take us far beyond the scope of a thesis to give a complete history of this problem, but it is appropriate to outline the essential events. To do so we rely upon several secondary sources¹ but where possible the original references will be cited. We begin by tracing the study of two separate physical phenomena: the photoelectric effect and the blackbody radiation distribution.

Every student of physics knows that James Clerk Maxwell synthesized the concepts of electricity and magnetism.² In the process oscillating fields which propagated at the velocity of light were predicted and were subsequently observed by Heinrich Herz.³ Herz's experiments detected the near field radiation of a spark discharge and, at the time, he observed that the induced spark occurred more readily when the light from the source was allowed to fall on the secondary electrodes.⁴ This

phenomenon was studied until by 1905 almost all of the details of the photoelectric effect were well known to physicists.

The study of blackbody radiation is obscured somewhat by our lesser familiarity with the thermodynamics required for its study. In 1859 G. R. Kirchhoff⁵ proved that the ratio of the emission of heat to absorption was independent of the nature of the body involved. With the invention of the bolometer by S. P. Langley⁶ the study of the wavelength distribution of cavity radiation could proceed on a firm experimental basis. In the meantime, theoretical considerations had verified Stefan's law^{7,8} and established what is now known as Wien's displacement law.⁹

All this was done without trying to understand the detailed processes involved. As a first attempt at dealing with the underlying interaction Wien derived, on rather weak physical assumptions, a distribution law for the radiated energy:

$$u_{\nu} = \alpha \nu^3 e^{-\beta \nu / T}, \quad (1)$$

where u_{ν} is the radiation density in the frequency

interval ν to $\nu + d\nu$, T is the absolute temperature, and α and β are constants. This was subsequently put on firmer ground by Max Planck.¹⁰ At the same time the Rayleigh distribution law,

$$u_\nu = 8\pi\nu^2 kT/c^3 \quad (2)$$

was proposed. Equations 1 and 2 each agreed with parts of the data available, but violently disagreed with the rest.

To fully understand the resolution of the problem would require an excessive digression into classical thermodynamics, so we simply state the results. A fundamental relation for any constant volume thermodynamic system is

$$\partial S/\partial U = T^{-1} \quad (3)$$

where S is the entropy of the system and U is the internal energy. The physics enters when we write U as a function of T . The different radiation laws involve the equilibria predicted by two forms for the second derivative:

$$\partial^2 S/\partial U^2 \propto U^{-1} \quad (4a)$$

versus

$$\partial^2 S/\partial U^2 \propto U^{-2}. \quad (4b)$$

The first leads to the Wien law and the second to

Rayleigh's. The compromise was obvious;

$$\partial^2 S / \partial U^2 \propto 1/U(b + U), \quad (5)$$

but what justification could be given? Planck was forced to use Boltzmann's statistical interpretation of entropy from which equation 5 followed if the distribution of energy to the radiators was discrete. The quantum was born, albeit reluctantly.¹¹ It should be noted at this point it is matter which is quantized, not the radiation.

In 1905 Einstein succeeded in bringing these two phenomena together by transferring the discreteness of the energy distributions to the radiation.¹² The excitement with which this was received is summed up by Planck in his nominating statement for Einstein's admission to the Prussian Academy in 1913:

"That he may sometimes have missed the target in his speculations, as for example, in his hypothesis of light quanta, cannot be held against him, for it is not possible to introduce fundamentally new ideas, even in the most exact sciences, without occasionally taking a risk."

The "photon" would not go away, however. By 1916 Millikan had painstakingly verified all the predictions for the photoelectric effect,¹³ and in 1923 the

Compton effect¹⁴ was explained in terms of a "particle-particle" interaction. In the meantime, the understanding of matter had also changed.

The description of atomic processes made incredible progress during this period if one considers that most of the models were purely speculative. As an example of the "old quantum theory", the Landé g-values¹⁵ were established by assigning to the core of the atom an angular momentum which corresponds to our electron spin. Hence, the persistence in German of calling j the "inner quantum number". Basically, the old quantum theory took the Bohr atom, the correspondence principle, and the established formalism for solving multiply periodic motions to explain the experimental data which had accumulated in atomic physics. It remained for a group of young physicists, born at the same time as the quantum, to provide a quantum mechanics.

For our purposes quantum mechanics has two formulations: matrix mechanics and wave mechanics; the principal parts of the latter overlapped the former. The first modern wave mechanics was developed by

L. de Broglie in a series of papers in 1923 and presented as a doctoral thesis in 1925. The only points that we need be aware of are that the work is done in the framework of special relativity and that one must understand the distinctions between group and phase velocity to treat the theory correctly. With this model de Broglie was able to solve the Bohr hydrogen atom from first principles and suggest to his brother that he look for electron diffraction. (The laboratory was too busy trying to invent television to do so.)

The matrix mechanics begins with W. Heisenberg.¹⁶ Heisenberg was a strong advocate of the discontinuity of all microscopic processes.¹⁷ As a consequence he was willing to reject the notion of a well-defined trajectory, and looked for a way to make position and momentum quantum mechanical variables in the same sense as the energy. The results led to a matrix mechanics which also predicted the experimentally known results for the hydrogen atom and the anharmonic oscillator. The full formalism is found in the papers by Born and Jordan¹⁸ and Born, Jordan and Heisenberg.¹⁹ These papers allow

quite accurate descriptions of atomic phenomena; once again, from first principles.

At this point E. Schroedinger published a sequence of papers²⁰⁻²³ which established the wave mechanics as an outgrowth of the Hamilton-Jacobi theory. Starting with a generating function

$$S = K \ln \Psi \quad (6)$$

in the Hamilton equation

$$H(q, \partial S / \partial q) = E \quad (7)$$

he reduced the quantization of the hydrogen atom to an eigenvalue problem for the time independent Schroedinger equation. With this done he then solved the harmonic oscillator, established the wave mechanical nature of the theory, produced the necessary perturbation theory, arrived at a time dependent equation, and, in an intervening paper,²⁴ showed the formal identity of matrix mechanics to wave mechanics. Since it gave an analytic method for obtaining a description of physical systems the wave mechanics soon became the way to solve problems and by 1930 most of the standard results had been obtained.¹⁷

In the meantime, the existence of a proper quantum treatment of the harmonic oscillator permitted the photon to become a full physical theory²⁵ rather than a heuristic device. Implicit in Dirac's development was an operator formalism which of its nature precludes the study of the instantaneous matter-radiation interaction. While we could trace the history of quantum electrodynamics into the forties,²⁶⁻²⁸ we have reached the point at which this experiment fits.

What of the coupling of matter and radiation? This involves our interpretation of Ψ and, more importantly, just what we expect our description of nature to accomplish. Those who wish philosophical discussions of measurement theory are referred elsewhere,²⁹⁻³¹ but we must treat some of the problem here since the philosophical implications determine how we cut metal.

Schrödinger felt initially that $e\Psi\Psi^\dagger$ represented the charge density in configuration space²³ and he showed briefly how to arrive at the oscillator strengths from this standpoint.²⁴ The difficulty with this is apparent in two related ways. Firstly, the temptation is to keep the notion of trajectory by looking at wave packets.

This runs counter to the ascendant philosophical notion that what is not observable must not be included in the theory, although the complete elimination of continuous processes did not occur until the fifth Solvay Conference. More importantly, wave packets do not work in the solution of collision problems since the packet always spreads out--with the exception of the harmonic oscillator functions used by Schroedinger to test the concept.

Born, at the time, was working in the same building as Franck. As a result he firmly believed that the correct interpretation could leave no fuzziness about the nature of an observed electron: it was a particle. Returning to de Broglie's guide wave concept he interpreted $\Psi\Psi^\dagger$ as giving the probability density of finding the actual particle at the point in configuration space³² involved, and developed the Born approximation for describing collisions.³³ While Schroedinger pointed out that such an interpretation required an additional hypothesis to his development,³⁴ the interpretation was too fruitful to be rejected.

The fundamental problem here is psychological, although it may be couched in epistemological terms. The

strict probabilistic interpretation of quantum mechanics requires that we give up knowing or even talking about how one event leads to another, even though we have a definite prescription for predicting the possible sequences of events. Bohr covered this difficulty with the principle of complementarity, but the problem always reverts to our basic notion of what it means "to understand". If one can attach a dynamical significance to Ψ then he understands in a more satisfying sense than if he only calculates ensemble probability averages. Those influenced directly by Bohr and hence by the philosophies of Kierkegaard and James³⁵ were able to sublimate these difficulties, but each generation of students must face them anew.

A second, more physical problem, arises from the nature of modern quantum electrodynamical theory. It works well,³⁶ but often appears to sweep difficulties away in a manner reminiscent of the old quantum theory.

The experiment described below looks at an alternative to the canonical interpretation. The photon, whether accepted or not, was part of the world for over twenty years before the quantum theory of matter was

workable. Is it not possible that all photon effects are really in the quantized eye of the beholder? Such explanations account for the photoelectric effect³⁷ and a number of other supposed QED effects.³⁸ By the same token, a return to the Schroedinger interpretation of Ψ would give time varying sources to produce radiation.

Such a theory--more appropriately, a philosophy--has been advanced by E. T. Jaynes and his collaborators.³⁹⁻⁴¹ We propose a direct test of this theory. In the process we will also be able to look for limitations on the exponential decay law. To fix in the reader's mind this purpose, we digress here to give an overview of the experiment.

The Jaynes' theory predicts a radiative decay law which differs from that of QED. For the excited state densities available to us this would be observed as a linear variation in the lifetime of the $2p_{1/2}$ state as a function of the presence of the metastable $2s_{1/2}$ state. To observe this, a beam of 60 keV hydrogen atoms was produced which consisted of about 10% atoms in the metastable state. (We use the usual beam interpretation here.) If a controlled fraction of these was converted to the $2p_{1/2}$ state

by a short electrical pulse, the subsequent radiation could be monitored to directly measure the changes in the lifetime.

We begin now by looking at the predictions of QED and the Jaynes' theory concerning the behavior of atomic systems.

CHAPTER II
RADIATION THEORY I
QUANTUM ELECTRODYNAMICS

The statement "light exists as photons" does not alone make a quantum electrodynamics. Between the proposal in 1905 that light must be treated as energy quanta^{1,2} and the full quantization^{2,5} of the radiation field in 1927 no proper formalism could be generated for the simple reason that no well defined quantum mechanical structure existed. As soon as an acceptable theory of the harmonic oscillator^{1,6,2,1} was developed the photon^{4,2} was established as part of a working physical theory. Let us now derive the exponential decay law in terms of this theory for the atomic system used in these experiments.

We consider a volume of space Ω containing an ensemble of atoms and electromagnetic radiation. The atoms obey a Hamiltonian H_0 which generates stationary states in the absence of the radiation field:

$$H_0 \phi_k(\vec{r}) = \omega_k \phi_k(\vec{r}). \quad (1)$$

(Throughout this paper, the convention $\hbar = 1 = c$ is used, so that energies, frequencies and wave numbers may be used interchangeably.)

The radiation fields are source free and completely described by a transverse vector potential \vec{A} . (This is more carefully treated in chapter III.) \vec{A} is to be written in terms of photon states. Consider the possibilities: The "finite" volume Ω defines a lattice of possible wave vectors \vec{k} , each of which may have two orthogonal polarizations $\hat{e}(\vec{k}, \lambda)$. Each of these may be "occupied" by 0, 1, 2... photons. To produce a dynamics, raising and lowering operators, $a^\dagger(\vec{k}, \lambda)$ and $a(\vec{k}, \lambda)$ are defined which have the following properties: Let $|\cdots N(\vec{k}, \lambda) \cdots\rangle$ correspond to a photon state in which there are N photons of wave vector \vec{k} and polarization λ along with other unchanging occupations. Then

$$a^\dagger(\vec{k}, \lambda) |\cdots N(\vec{k}, \lambda) \cdots\rangle = \sqrt{N+1} |\cdots (N+1)(\vec{k}, \lambda) \cdots\rangle, \quad (2)$$

$$a(\vec{k}, \lambda) |\cdots N(\vec{k}, \lambda) \cdots\rangle = \sqrt{N} |\cdots (N-1)(\vec{k}, \lambda) \cdots\rangle, \quad (3)$$

and

$$a^\dagger(\vec{k}, \lambda) a(\vec{k}, \lambda) |\cdots N(\vec{k}, \lambda) \cdots\rangle = N |\cdots N(\vec{k}, \lambda) \cdots\rangle. \quad (4)$$

This last combination is called the number operator and is used to generate the radiation Hamiltonian.

It then follows that⁴³

$$\vec{A} = \sum_{\vec{k}, \lambda} \sqrt{2\pi/\Omega k} \{ a(\vec{k}, \lambda) e^{i\vec{k} \cdot \vec{r}} + a^\dagger(\vec{k}, \lambda) e^{-i\vec{k} \cdot \vec{r}} \} \hat{\epsilon}(\vec{k}, \lambda), \quad (5)$$

where the operator amplitudes contain an implicit time dependence:

$$a(\vec{k}, \lambda) = a(\vec{k}, \lambda) |_{t=0} e^{-ikt}.$$

Note that \vec{A} is transverse:

$$\nabla \cdot \vec{A} = 0.$$

The energy of our portion of the world is

$$E = (\frac{1}{2}m) \{ \vec{p} + e\vec{A} \}^2 + \phi_{\text{atomic}} + E_{\text{rad}}, \quad (6)$$

so that to first order in \vec{A} the perturbed atomic Hamiltonian is

$$H = H_0 + (e/m) \vec{A} \cdot \vec{p} = H_0 + V. \quad (7)$$

Here, $-e/m$ is the electronic charge to mass ratio.

Hence,

$$V = (e/m) \sum_{\vec{k}, \lambda} \sqrt{2\pi/\Omega k} \{ a(\vec{k}, \lambda) e^{i\vec{k} \cdot \vec{r}} + a^\dagger(\vec{k}, \lambda) e^{-i\vec{k} \cdot \vec{r}} \} \vec{p} \cdot \hat{\epsilon}(\vec{k}, \lambda) \quad (8)$$

is the perturbing potential.

In our work we will be populating three atomic states: $\phi_1(\vec{r})$ will be the ground state; $\phi_2(\vec{r})$ will lie

$\omega_0 + \omega$ above ϕ_1 but not coupled to it by V ; and $\phi_3(\vec{r})$ will lie ω above ϕ_1 and be coupled to both ϕ_2 and ϕ_1 . Further, $\omega_0 \ll \omega$. These are illustrated in figure one. Initially the atom will be in a mixture of ϕ_2 and ϕ_3 with no photons in the radiation field. The general state will then be

$$\begin{aligned} \Psi(\vec{r}, t) = & \sum_{\vec{k}, \lambda} c_1(\vec{k}, \lambda; t) e^{-i\vec{k}t} \phi_1(\vec{r}) |\vec{k}, \lambda\rangle \\ & + c_2(t) e^{-i(\omega_0 + \omega)t} \phi_2(\vec{r}) |\phi\rangle \\ & + c_3(t) e^{-i\omega t} \phi_3(\vec{r}) |\phi\rangle, \end{aligned}$$

where $|\vec{k}, \lambda\rangle$ designates the existence of one photon of wave vector \vec{k} and polarization λ and no others, and $|\phi\rangle$ is the vacuum state. The initial conditions are

$$c_1(\vec{k}, \lambda, 0) \equiv 0 \tag{9a}$$

$$|c_2(0)|^2 + |c_3(0)|^2 = 1. \tag{9b}$$

The Schroedinger equation gives

$$\begin{aligned} i\dot{c}_1(\vec{k}, \lambda; t) = & \\ & \sqrt{2\pi/\Omega k} (e/m) \hat{\epsilon}(\vec{k}, \lambda) \cdot \langle 1 | e^{-i\vec{k} \cdot \vec{r}} | 3 \rangle e^{-i(\omega - k)t} c_3(t), \end{aligned} \tag{10}$$

$$i\dot{c}_2(t) = 0, \tag{11}$$

and

$$i\dot{c}_3(t) = \sum_{\vec{k}, \lambda} \sqrt{2\pi/\Omega k} (e/m) \hat{\epsilon}(\vec{k}, \lambda) \cdot \langle 3 | e^{i\vec{k} \cdot \vec{r}_p} | 1 \rangle e^{i(\omega-k)t} c_1(\vec{k}, \lambda; t). \quad (12)$$

The coupling between states Φ_2 and Φ_3 has been ignored since, as we shall see, it is down by a factor of 10^{18} over the other coupling. To this approximation, we have a linear two state problem; the presence of residual "metastable" atoms does not affect the behavior of the radiating state.

To solve the system of equations we use the fact that $c_1(\vec{k}, \lambda; 0) \equiv 0$ to obtain

$$c_1(\vec{k}, \lambda; t) = -i\sqrt{2\pi/\Omega k} (e/m) \{ \hat{\epsilon}(\vec{k}, \lambda) \cdot \langle 1 | e^{-i\vec{k} \cdot \vec{r}_p} | 3 \rangle \} \times \int_0^t c_3(\tau) e^{-i(\omega-k)\tau} d\tau,$$

which, in turn, is to be substituted into equation 12.

The equivalence

$$\sum_{\vec{k}} \rightarrow (\Omega/8\pi^3) \int d^3k$$

gives

$$i\dot{c}_3(t) = - \int_0^t e^{i\omega(t-\tau)} c_3(\tau) \int_0^\infty |V(k)|^2 e^{-ik(t-\tau)} dk d\tau \quad (13)$$

where

$$|V(k)|^2 = (e/m)^2 (k/4\pi^2) \sum_{\lambda} \int d\Omega_k |\langle 1 | e^{-i\vec{k} \cdot \vec{r}} \vec{p} \cdot \hat{\epsilon}(\vec{k}, \lambda) | 3 \rangle|^2 \quad (14)$$

is called the form factor.

Several possibilities present themselves. An exact solution is possible in principle. The expression in equation 13 can be made into a convolution and $c_3(t)$ obtained by Laplace transforms. The result is exponential decay with several shortlived transients and a small asymptotic t^{-2} behavior. Another alternative is to do a dipole approximation to $|V(k)|^2$ and then proceed "exactly". The traditional approach⁴⁴ has been to make the dipole approximation and to assume exponential decay:

$$c_3(t) \propto e^{-\frac{1}{2}\Gamma t} \quad (15)$$

The rate Γ is adjusted to achieve self consistency in equation 13 for times great compared to ω^{-1} . This is sufficient for our purposes.

Equation 13 is now

$$\begin{aligned} \frac{1}{2}\Gamma e^{-\frac{1}{2}\Gamma t} &\approx \int_0^t e^{i\omega(t-\tau)} e^{-\frac{1}{2}\Gamma\tau} \int_0^{\infty} |V(k)|^2 e^{-ik(t-\tau)} dk d\tau \\ &= ie^{-\frac{1}{2}\Gamma t} \int_0^{\infty} |V(k)|^2 \left\{ \frac{1 - e^{i(\omega-k-\frac{1}{2}i\Gamma)t}}{\omega - k - \frac{1}{2}i\Gamma} \right\} dk, \end{aligned} \quad (16)$$

and since $\Gamma \ll \omega$ we have

$$\begin{aligned} \frac{1}{2}\Gamma &\approx \int_0^\infty \{\sin(\omega-k)t/(\omega-k)\} |V(k)|^2 dk + \\ &i \int_0^\infty \{(1 - \cos(\omega-k)t)/(\omega-k)\} |V(k)|^2 dk. \end{aligned} \quad (17)$$

For $\omega t \gg 1$ the oscillatory parts of the integrands have the effect of sharply defining the region about ω .⁴⁵ The real part becomes

$$\text{Re}\Gamma = \gamma = 2\pi \int_0^\infty \delta(\omega-k) |V(k)|^2 dk = 2\pi |V(\omega)|^2. \quad (18)$$

Finally, in the dipole approximation

$$\begin{aligned} |V(\omega)|^2 &\approx (\omega/4\pi^2) \sum_\lambda \int d\Omega_k |\langle 1 | [H, \vec{\mu}] | 3 \rangle \cdot \hat{\epsilon}(\vec{k}, \lambda)|^2 \\ &= (2\omega^3/3\pi) |\mu_{13}|^2. \end{aligned}$$

where $\vec{\mu}$ is the electronic dipole moment. Hence,

$$\gamma \approx (4\omega^3/3) |\mu_{13}|^2. \quad (19)$$

The atomic system will radiate energy at a rate

$$R = - \frac{d}{dt} |c_3(t)|^2 \omega = \omega \gamma |c_3(0)|^2 e^{-\gamma t}, \quad (20)$$

an expression which is generally accepted as true and which is tested here. We now turn to a somewhat different analysis of the same problem.

Figure one: Three level atom. This idealized hydrogen structure forms the basis for the research done. A full radiation theory must predict ω_0 since the upper levels are degenerate in the ordinary atomic theory. For the work here the levels should be identified with the hydrogenic $1s_{\frac{1}{2}}$, $2s_{\frac{1}{2}}$ and $2p_{\frac{1}{2}}$ levels, respectively.

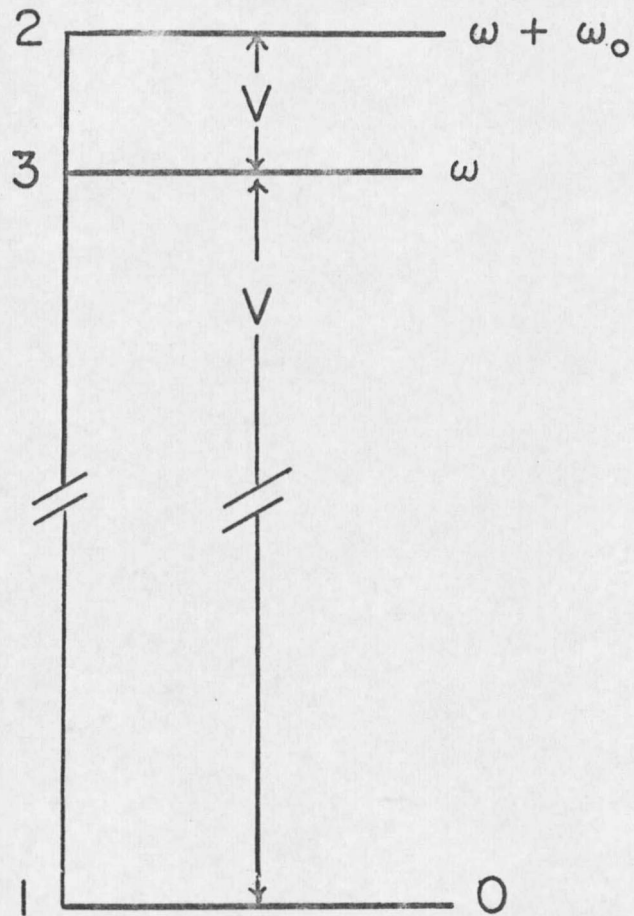


FIG 1

CHAPTER III
RADIATION THEORY II
SEMICLASSICAL THEORY

A complete quantum theory of radiation was not uniquely difficult. The consistent treatment of the interaction of classical electromagnetic fields and matter was not fully accomplished until the 1960s.⁴⁶ The interaction of classical fields and quantized matter has been studied for an equal period and the reader is directed to the review article by Scully and Sargent for a bibliography.³⁸ We concern ourselves here with the developments of E. T. Jaynes and his students,³⁹⁻⁴¹ although we shall use an exposition which follows a slightly different approach.⁴⁷

The semiclassical radiation theory (SCT) of Jaynes differs from earlier treatments⁴⁸ in that it studies the dynamics of the interaction in detail. This is done at the expense of the standard interpretation of $\Psi^\dagger\Psi$ as a probability density over an ensemble of identical atoms. Rather, SCT follows Schroedinger's original notion that

$$\rho = -e\Psi^\dagger\Psi \quad (1)$$

is the electronic charge density in configuration space.⁴⁹ For a single electron atom this is a real spatial charge distribution. From this and the usual notion of continuity, the current density is

$$\vec{j} = \text{Re}\{(-e/m)(\Psi^\dagger \vec{p} \Psi)\}. \quad (2)$$

These are point functions, not matrix elements, and act as sources for electromagnetic fields.

This drastically differs from the QED starting point. There the fields derive from photon states which exist independently of the atom. The current density matrix element determines the coupling to the photon states, but cannot be said to be responsible for their existence. One implication of this difference can be seen quickly. Let us assume we have a dipole transition which would couple the states of a two level atom. In QED if an ensemble of atoms were initially in the excited level, we would see radiation immediately with a rate given by

$$R = N\omega\gamma e^{-\gamma t}, \quad (3)$$

where ω is the energy separation of the states and

$$\gamma = (4/3)\mu^2\omega^3. \quad (4)$$

The dipole strength enters only as the matrix element

$$\mu^2 = |\langle 1 | -e\vec{r} | 2 \rangle|^2. \quad (5)$$

For an SCT treatment, as we shall see, the radiation rate depends on a physically oscillating dipole and to the same approximation we observe at a large distance,

$$R \propto \left| \int \Psi^{\dagger} \vec{\mu} \Psi d^3 r \right|^2. \quad (6)$$

If Ψ is initially in a single parity state this vanishes. Spontaneous decay can occur only if there is some residual ground state present to give a nonvanishing dipole to initiate the process. This clearly precludes a purely exponential decay. The reason such behavior is not observed stems from the impossibility of producing pure excited states.

This point is tricky. In SCT when we speak of an atomic beam which consists of say 12% atoms in some state, Φ_{α} , we do not mean that 12% of the atoms are in the state Φ_{α} and the remaining 88% in other states. Rather, we mean that each atom has a wave function which on the average is 12% Φ_{α} . This makes the discrepancy from QED difficult to test. Most of the other possible problems are treated by Scully in his Physics Today review.³⁸ An effect does exist⁵⁰ which can be realized experimentally, as we shall now show.

The electric and magnetic field strengths at a point may be written in terms of longitudinal and transverse components:

$$\vec{E} = \vec{E}_\ell + \vec{E}_t \quad (7a)$$

$$\vec{B} = \vec{B}_t \quad (7b)$$

where

$$\nabla \cdot \vec{E}_t = 0, \quad (8a)$$

$$\nabla \times \vec{E}_\ell = 0, \quad (8b)$$

$$\nabla \cdot \vec{B}_t = \nabla \cdot \vec{B} = 0. \quad (8c)$$

In terms of these vectors and their sources Maxwell's equations are

$$\nabla \cdot \vec{E}_\ell = 4\pi\rho, \quad (9a)$$

$$\frac{\partial \vec{E}_\ell}{\partial t} = -4\pi\vec{j}_\ell, \quad (9b)$$

$$\nabla \times \vec{E}_t = -\frac{\partial \vec{B}_t}{\partial t}, \quad (9c)$$

and

$$\nabla \times \vec{B}_t = \frac{\partial \vec{E}_t}{\partial t} + 4\pi\vec{j}_t. \quad (9d)$$

Since it is the longitudinal part of \vec{E} which contains all the source dependence, \vec{E}_t and \vec{B}_t are sufficient to describe the radiation problem.⁵¹

This description is best carried out by introducing a vector potential $\vec{A}(\vec{r}, t)$ in the Coulomb gauge:

$$\nabla \cdot \vec{A} = 0 \quad (10a)$$

$$\vec{B}_t = \nabla \times \vec{A} \quad (10b)$$

$$\vec{E}_t = -\frac{\partial \vec{A}}{\partial t} \quad (10c)$$

When this is introduced into equation 9d we have

$$\{\nabla^2 - \frac{\partial^2}{\partial t^2}\} \vec{A} = -4\pi \vec{j}_t \quad (11)$$

for which the appropriate solution is

$$\vec{A}(\vec{r}, t) = -\int R^{-1} \vec{j}_t(\vec{r}', t-R) d^3 r' \quad (12)$$

where

$$R = |\vec{r} - \vec{r}'|. \quad (13)$$

The retarded solution is deliberately chosen since it is the only meaningful one in this context.

This expression must now be substituted into the Schroedinger equation with the Hamiltonian

$$H \approx H_0 - \vec{A} \cdot \vec{j}_t \quad (14)$$

where H_0 is the unperturbed atomic Hamiltonian and \vec{A} and \vec{j}_t are determined by equations 12 and 2. The result is a nonlinear theory, which is to be used to solve the same

problem as in chapter II with one difference: the two upper levels will be degenerate, $\omega_0 = 0$. This system and the couplings are shown in figure one.

The total wave function is written as

$$\begin{aligned} \Psi(\vec{r}, t) = & c_1(t)\phi_1(\vec{r}) + c_2(t)e^{-i\omega t}\phi_2(\vec{r}) \\ & + c_3(t)e^{-i\omega t}\phi_3(\vec{r}), \end{aligned} \quad (15)$$

and we are interested in the time evolution of the quantities

$$N(t) = \sum_i |c_i(t)|^2 \quad (16)$$

and

$$E(t) = \sum_i \omega_i |c_i(t)|^2. \quad (17)$$

where $N(t)$ is normalization of $\Psi(\vec{r}, t)$ and

$$H_0 \phi_i(\vec{r}) = \omega_i \phi_i(\vec{r}). \quad (18)$$

We now show that $N(t)$ is unity even when the atom radiates and then compare dE/dt with the same quantity in chapter II.

The Schroedinger equation gives

$$i\dot{c}_j(t) = - \sum_k c_k(t) e^{-i\omega_{kj}t} \int \phi_j^\dagger(\vec{r}) \vec{A} \cdot \vec{j}_t \phi_k(\vec{r}) d^3r \quad (19)$$

where

$$\omega_{kj} = \omega_k - \omega_j.$$

The current density given in equation 2 can also be written as

$$\vec{j}_t(\vec{r}, t) = i\Psi^\dagger(\vec{r}, t)[H, \vec{\mu}_t]\Psi(\vec{r}, t) \quad (20)$$

so that the full expansion of equation 19 is

$$\begin{aligned} \dot{c}_j(t) = & \\ & i \sum_k \sum_\ell \sum_m c_k(t) \omega_{jk} \omega_{\ell m} e^{-i\omega_{jk}t} e^{-i\omega_{\ell m}t} M(j, k; \ell, m) \end{aligned} \quad (21)$$

where

$$\begin{aligned} M(j, k; \ell, m) = & \\ & \iint d^3r d^3r' c_\ell(t-R) c_m^*(t-R) R^{-1} e^{i\omega_{\ell m}R} \{ \Phi_j^\dagger(\vec{r}) \vec{\mu}_t \Phi_k(\vec{r}) \} \cdot \\ & \cdot \{ \Phi_\ell^\dagger(\vec{r}') \vec{\mu}_t \Phi_m(\vec{r}') \}. \end{aligned} \quad (22)$$

The first thing to do is eliminate the oscillating terms. The form of equation 21 is such that we may ignore the degeneracy and obtain

$$\dot{c}_j(t) = i \sum_k c_k(t) \omega_{jk}^3 M(j, k; j, k). \quad (23)$$

To evaluate the expressions in equations 16 and 17 we need to find

$$\frac{d}{dt} |c_j(t)|^2 = \dot{c}_j^* c_j + c_j^* \dot{c}_j. \quad (24)$$

We use equation 23 to evaluate this with two further approximations: The variation of $c_j(t)$ over the time in

the integration of the retardation is negligible, and we may also use

$$(\sin \omega_{jk} R) / (\omega_{jk} R) \approx 1. \quad (25)$$

Then we find

$$\frac{d}{dt} |c_j(t)|^2 = - \frac{4}{3} \sum_k |c_k(t)|^2 \omega_{jk}^3 |\mu_{jk}|^2 |c_j(t)|^2. \quad (26)$$

Here, μ_{jk} is the total dipole matrix element; the transverse part has been extracted by integrating over all solid angles relative to the direction of propagation of the radiation.

Because $\omega_{jk} = -\omega_{kj}$ we see that

$$\frac{dN(t)}{dt} \equiv 0$$

so that an initially normalized wave function will remain so. For our problem we find

$$\frac{dE(t)}{dt} = - \frac{4\omega^4}{3} |\mu_{31}|^2 |c_1(t)|^2 |c_3(t)|^2, \quad (27)$$

which differs from the QED result in that both the initial and final state amplitudes affect the rate.

The solution of the coupled equations in equation 26 is a straight forward exercise. We first introduce a density matrix notation

$$\sigma_{k\ell}(t) = c_k(t) c_\ell^*(t), \quad (28)$$

and then write

$$\dot{\sigma}_{11}(t) = \gamma \sigma_{11}(t) \sigma_{33}(t), \quad (29a)$$

$$\dot{\sigma}_{22}(t) = 0, \quad (29b)$$

$$\dot{\sigma}_{33}(t) = -\gamma \sigma_{33}(t) \sigma_{11}(t), \quad (29c)$$

where

$$\gamma = (4\omega^3/3) |\mu_{13}|^2$$

is the same characteristic rate as in QED. These coupled equations are subject to the conditions

$$\sigma_{11}(t) + \sigma_{22}(t) + \sigma_{33}(t) = 1 \quad (30a)$$

and

$$\sigma_{22}(0) = \sigma_2. \quad (30b)$$

We can solve equation 29b and then use equation 30a to eliminate $\sigma_{11}(t)$ from equation 29c:

$$\dot{\sigma}_{33}(t) = -\gamma \sigma_{33}(t) \{\eta - \sigma_{33}(t)\}, \quad (31)$$

where

$$\eta = 1 - \sigma_2. \quad (32)$$

This integrates to

$$\eta \gamma (t - t_0) = \ln\{\eta - \sigma_{33}(t)\} / \sigma_{33}(t) \quad (33)$$

where

$$\eta \gamma t_0 = \ln\{\sigma_{33}(0) / \sigma_{11}(0)\}. \quad (34)$$

Hence,

$$\sigma_{33}(t) = \eta / (1 + e^{\eta\gamma(t-t_0)}). \quad (35)$$

The presence of the residual metastable component and the initial excited state population both affect the time evolution of the system. The time t_0 in a typical experiment where

$$\sigma_{33}(0)/\sigma_{11}(0) \approx 0.1$$

and

$$\eta \approx 1$$

is

$$t_0 \approx -2.3/\gamma$$

so that $\sigma_{33}(t)$ is described by its asymptotic behavior

$$\sigma_{33}(t) \sim \eta \{ \sigma_{33}(0)/\sigma_{11}(0) \} e^{-\eta\gamma t}. \quad (36)$$

We expect to see exponential decay, but both the rate and the apparent initial population are affected by a quantity which was totally irrelevant in the QED derivation. It is on the basis of this prediction that we can test SCT, for we can produce a beam of atomic hydrogen with a metastable component of about ten percent. By dumping different fractions of these into the $2p_{1/2}$ state and looking at the

subsequent decay rate we shall be able to look for changes in the rate as a function of σ_2 after the dump. The next two chapters describe the apparatus necessary; and the results appear in chapter VI.

CHAPTER IV

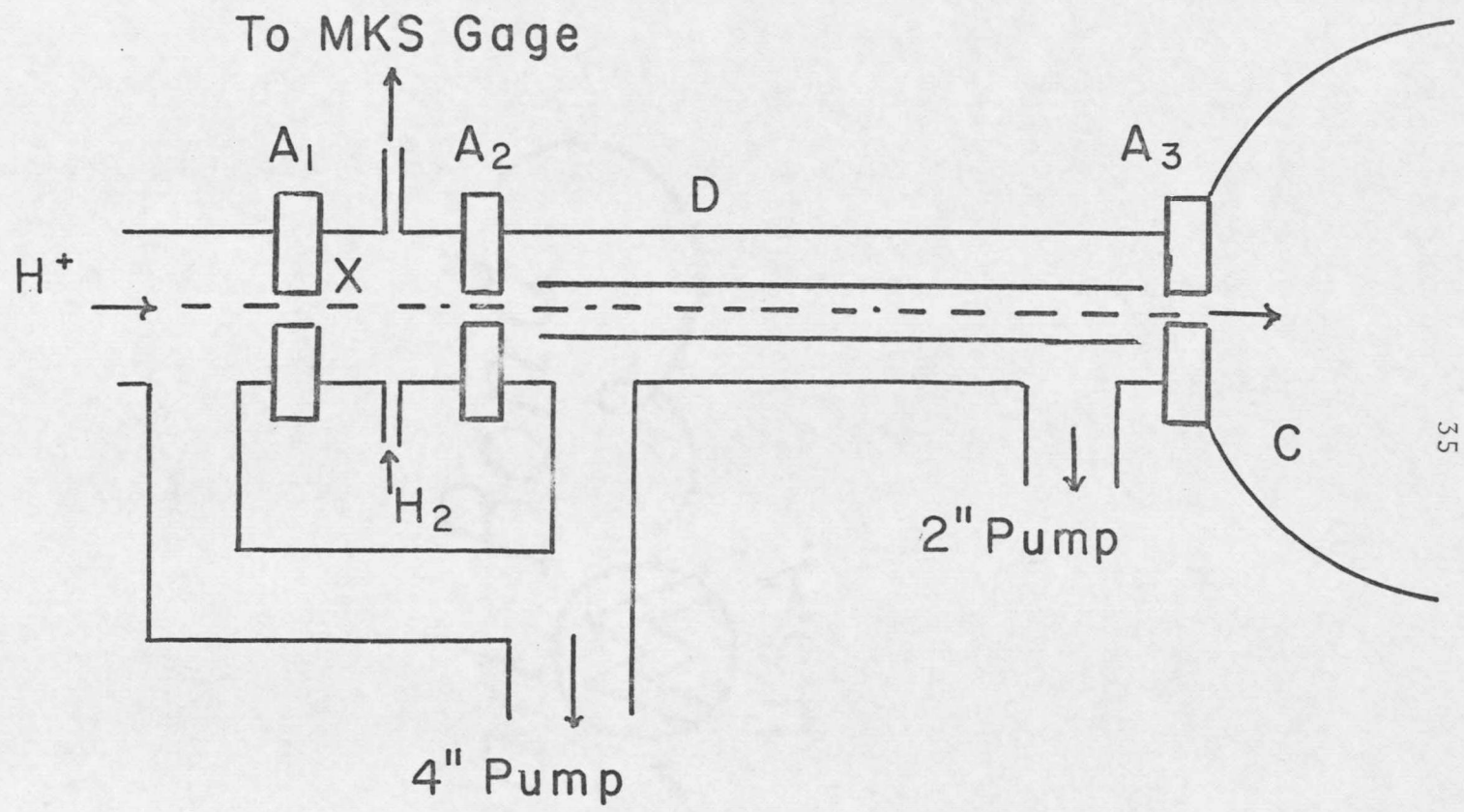
APPARATUS

So much for the nature of the problem; now to the equipment designed to test it. This apparatus was required to produce a well-collimated beam of hydrogen atoms with a known velocity and metastable fraction. It had to convert a variable fraction of the metastables into the $2p_{1/2}$ state in a time short compared to the $2p_{1/2}$ lifetime and without significantly populating any other states; and it was equipped to monitor the subsequent radiation in a statistically reliable way. The conversion problem will be treated in the following chapter; the rest of the apparatus is the subject here.

A prerequisite for a fast hydrogen beam is a fast proton beam. This was produced by a Cockcroft-Walton accelerator and analyzing system described elsewhere.⁵² Figures two and three show the rest of the system.

At the entrance to the charge exchange cell X, the 60 keV protons entered a region containing H_2 gas at a pressure of about 3.0μ where approximately 20% picked up an electron and became neutral hydrogen in some quantum state. From there the mixed beam entered a region D containing two parallel plates spaced 1.0 cm apart and

Figure two: Schematic view of the apparatus. The beam is collimated and mass analyzed when it enters the exchange cell (X). Differential pumping on either side of the exchange cell was accomplished by a 4" main diffusion pump operating on a manifold and assisted on the downstream side by a 2" pump. The "As" are the apertures.

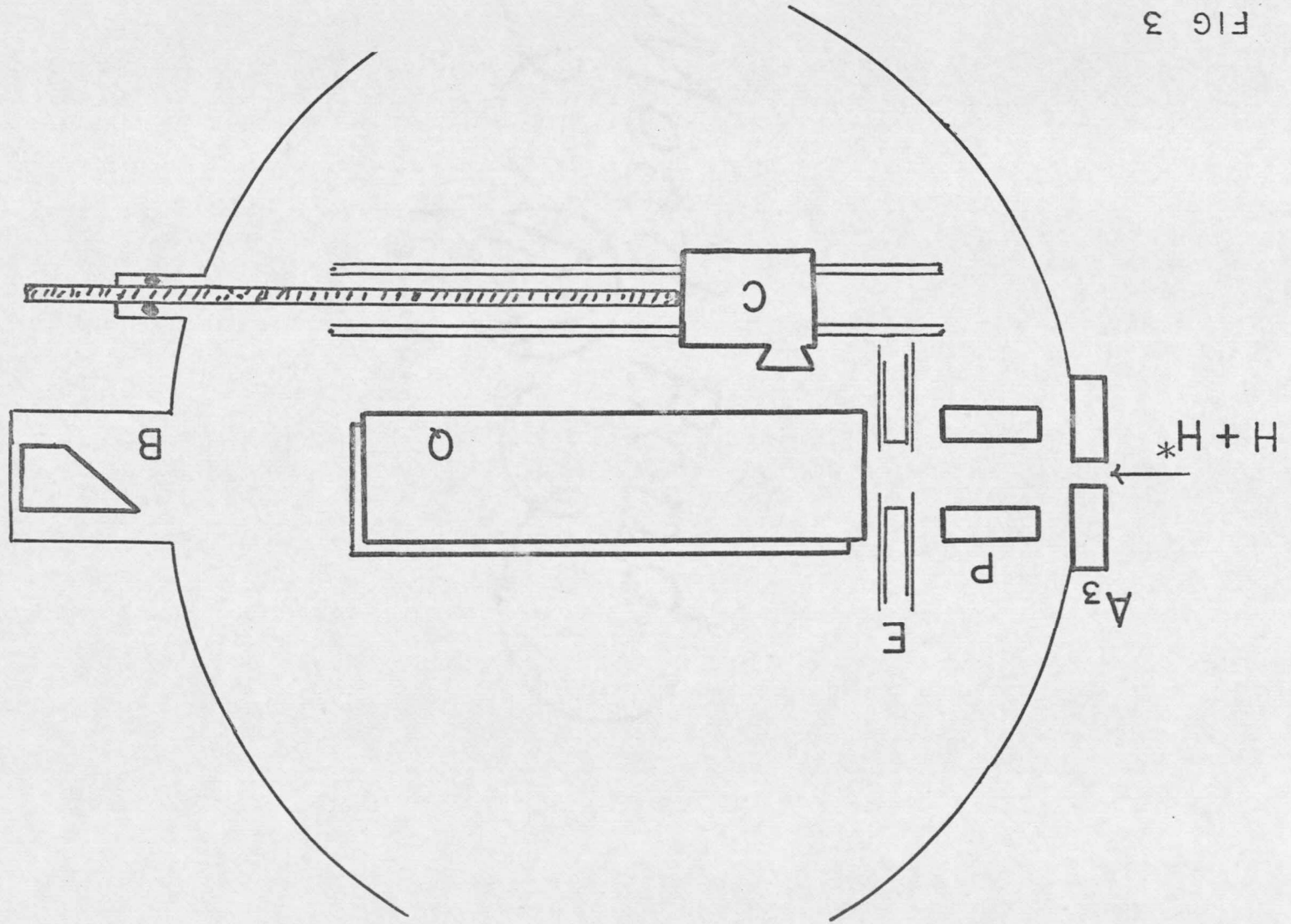


35

FIG 2

Figure three: Experimental chamber interior. For clarity the light collector (C) is shown as a cone; the actual geometry appears in figure nine. The beam monitor (B) detail is shown in figure twelve. The plates (Q) following the electrodes were added after the decay curves were taken.

FIG 3



39.5 cm long. These were charged just enough to sweep all the remaining protons from the beam. The pressure there was maintained at 5×10^{-6} T. Next the beam passed through an aperture into the experimental chamber C. The instrumentation there permitted the measurement of the radiation per atom and the indirect measurements of the 2p and 2s components of the beam. It consisted of a prequench electrode P, conversion electrodes E, a movable Lyman alpha detector C, and the beam current detector B. After the basic experiment was finished two long parallel plates Q were installed after the conversion electrodes for calibration purposes. These processes will now be discussed in detail beginning with the exchange cell.

The beam of protons entered the exchange region through a .041" movable aperture which further collimated the beam. The other end of the exchange cell had a similar aperture .036" in diameter and was located 10 cm downstream. The exchange cell gas, in this case H_2 , was admitted through a Granville Phillips Variable Leak and monitored by an MKS Baratron pressure meter referenced to the throat of the beam tube diffusion pump. The exchange cell pressure could be conveniently maintained between 0.5 and 10 μ . The systematic production of

metastable atoms required that beam atoms suffer only one collision. The graph in figure four illustrates the relative metastable production as a function of exchange cell pressure. The initial rise shows the gradual predominance of H_2 over the residual gases; the plateau is the single collision region; and collisional quenching becomes a factor thereafter. The differential pumping was not adequate to pursue the details⁵³ of this process.

The largest uncertainty in this experiment has to do with the percentage of the neutral beam in the metastable $2s_{1/2}$ state. Figure five shows this beam richness versus energy as inferred from the absolute cross section measurements of Bayfield.⁵⁴ Bayfield worked at exchange cell thicknesses on the order of 0.2 μ -cm, but the plateau shown in figure four justifies the 30 μ -cm value used to obtain a large count rate. He lists an uncertainty other than calibration of 20%. The potential calibration error is given as 55%. The least value for the richness consistent with other work⁵⁵ is about 2% at 30 keV. Since the destruction cross section seems to be decreasing⁵⁶ and the production is definitely increasing, it is appropriate to infer 2% as a lower limit but to quote results in terms of the 11.15% shown in figure five

Figure four: Exchange cell characteristics. The data taken over the first micron correspond to a mixture of H_2 and background gas. Beyond that the system is flushed. The nonlinearity at 3.0μ is approximately 10% as measured by the L_α counts per second.

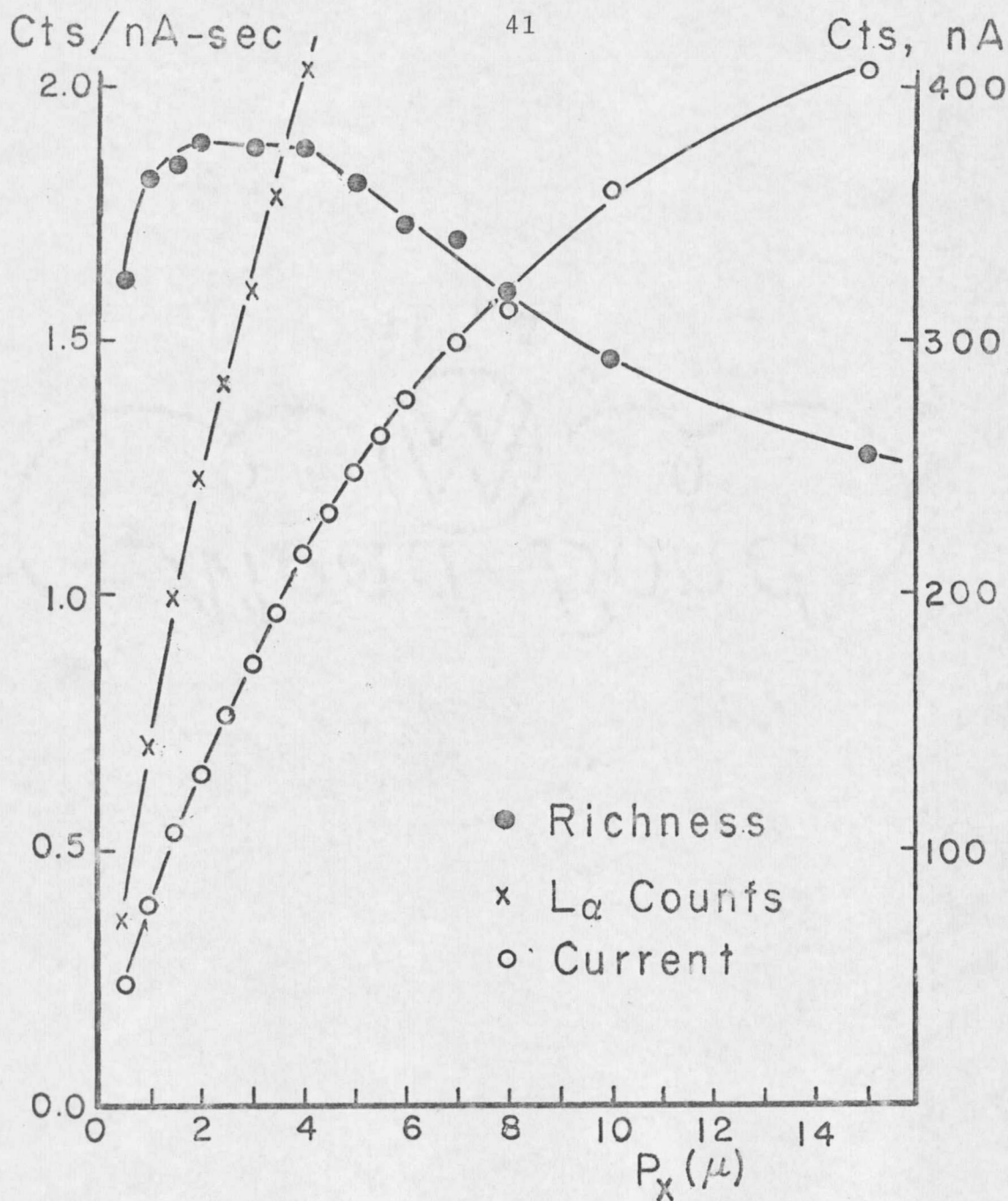


FIG 4

Figure five: Metastable fraction. The absolute cross section measurements given in reference fifty-four were used to infer the beam richness as a function of energy. The "richness" is defined as $\sigma_{2s}/\sigma_{\text{neutral}}$.

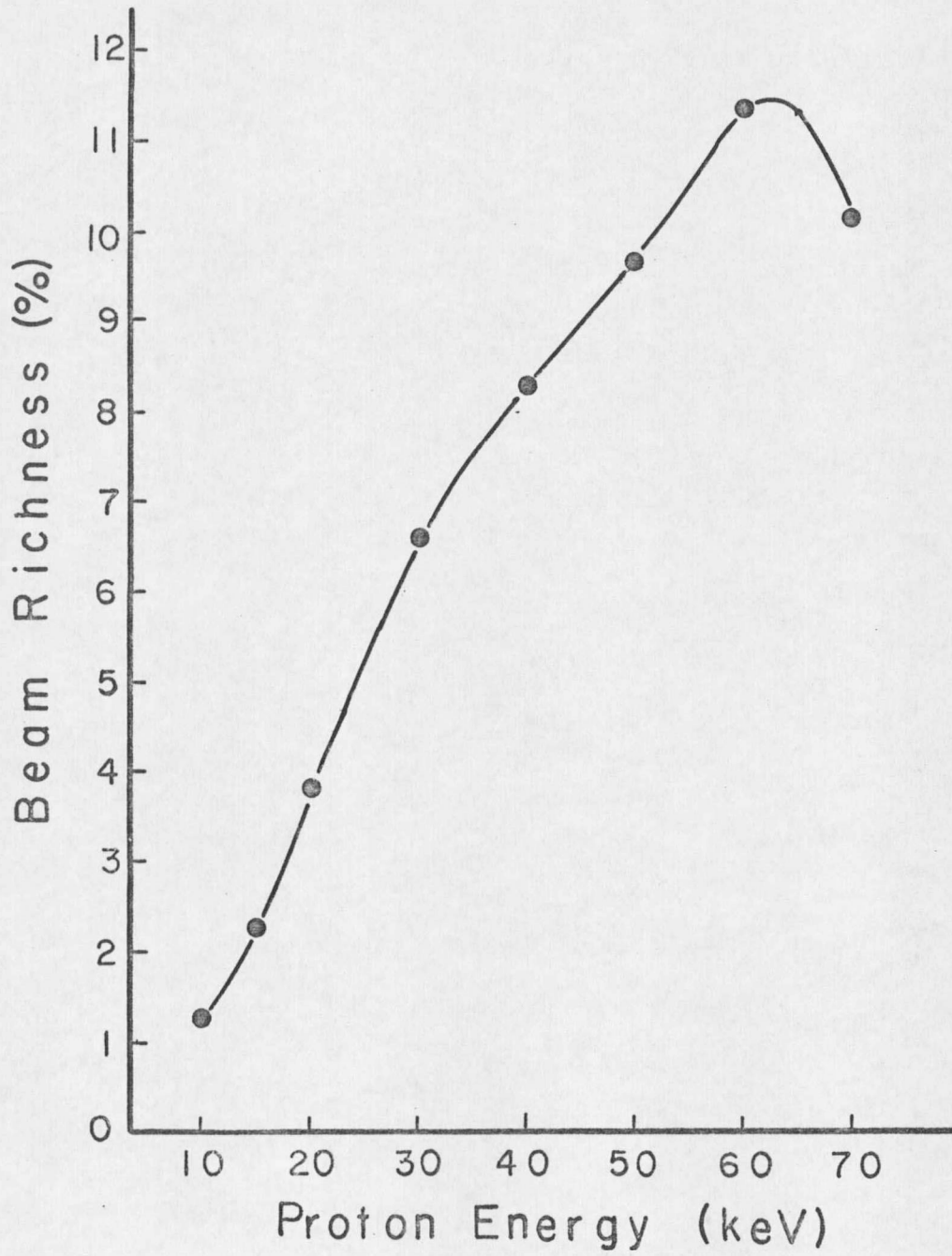


FIG 5

with a 20% uncertainty. As it happens the final results of the experiment are conclusive to well below a 1% level.

Upon leaving the charge exchange cell the mixed beam entered a long sweep region. Here an electric field of approximately 30 V/cm swept out all the residual protons. This was necessary since it was discovered that the presence of any protons destroyed the integrity of the counting statistics. This electric field is the smallest consistent with the requirement of pure Poisson statistics. The graph of the counting rate observed versus the potential across the plates shown in figure six is consistent with the low field limit developed in appendix A. From this graph it is seen that 78% of the metastables produced actually enter the experimental region through the last aperture.

This last aperture had a .020" hole which collimated the beam completely within the .041" hole in the electrode assembly. Each of these apertures could be grounded through an ammeter to help locate the beam. The three inches of beam tube prior to the first aperture was clear plastic so that at pressures around 10^{-4} T the actual shape of the beam there could be observed.

Figure six: Sweep destruction. By plotting the photon count rate as a function of the sweep voltage squared, the fraction of the metastable atoms destroyed in the sweep region was determined.

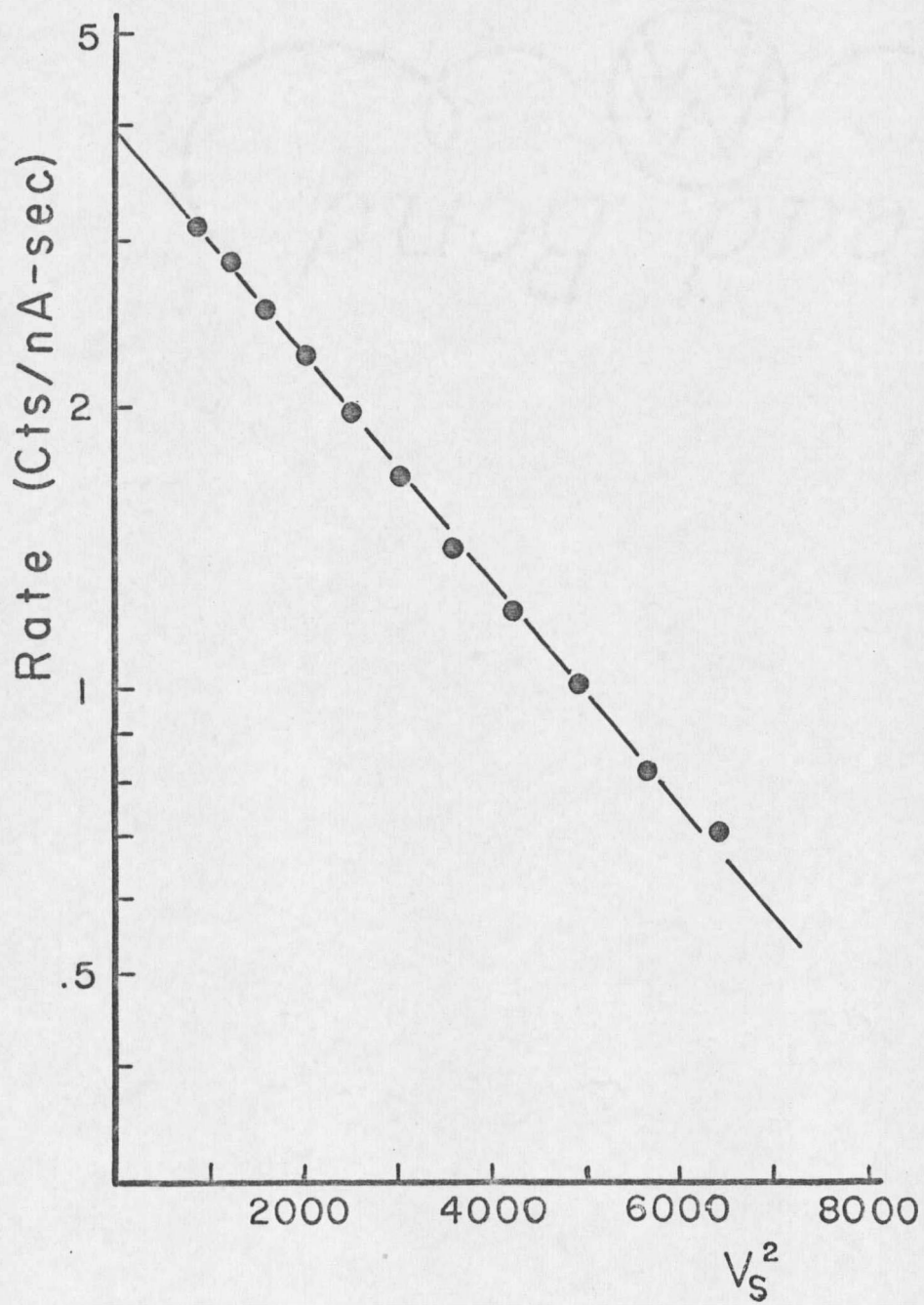


FIG 6

A schematic view of the experimental chamber is shown in figure three. All the parts were mounted on an aluminum plate which could be leveled and rotated for optimum alignment. The chamber itself was a 10½" ID by 6" brass pot which was mounted directly over the gate to a 4" diffusion pump system. The description of the parts follows in the order of their appearance to the beam.

The prequench electrode permitted the effects of a neutral ground state beam to be observed. It was a single flat piece of copper placed 0.83 cm below the top of a piece of square wave guide. (See figure seven.) When this was charged to about 1500 volts negative the two-inch length was sufficient to eliminate any metastables which might be observed. This prequench was used to differentiate between the background signal due to the beam presence alone and that caused by inadvertant quenching of metastables. It could also be used in the calibration process for the electrodes and the beam richness measurements shown in figures four and six. The background signal measured this way was very stable and was also position independent over about ten lifetimes along the beam.

Figure seven: Prequench electrode. The ground plane formed by standard .720" square waveguide was 0.83 cm above the copper electrode. The structure was 5 cm long, and the electrode was 1.82 cm wide.

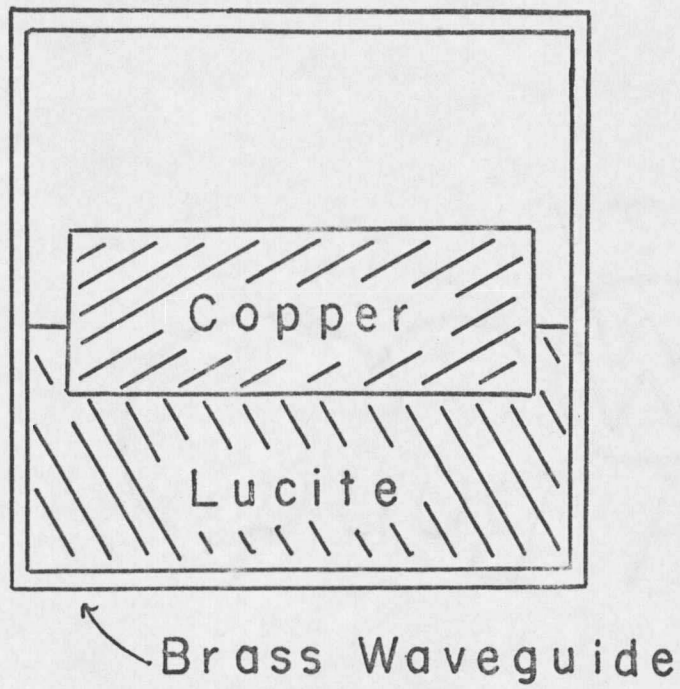


FIG 7

The electrode structure was located 2.5 inches downstream from the last aperture. The details of the actual electrode assembly are deferred to chapter V but some description is necessary for clarity. The assembly was constructed on a piece of .032" copper which was then mounted on a brass support. This support was $\frac{1}{4}$ " thick and isolated from ground by a piece of lucite. As a consequence the fraction of the beam which hit the structure could be determined to within a factor of two or three which is due to secondary electron emission characteristics. The beam at the third aperture was about two millimeters broad and as that aperture was moved across this profile a pronounced minimum was observed in the electrode current. With a secondary electron current at the beam detector of 200 nA the electrode "current" was held between 0.1 and 0.2 nA. The beam filled between 80 and 90% of the aperture.

The potential difference across the electrodes applied a short electrical pulse to the atoms. This converted, or mixed depending on the interpretation, some of the metastables into the $2p_{\frac{1}{2}}$ state. This fraction subsequently decayed to the ground state by

emitting Lyman alpha (L_{α}) radiation in the field free downstream region. The light was detected by a Bendix channeltron electron multiplier photon detector (CEM).

(The use of a "photon" detector to test a classical radiation theory was made possible by the fact that the photoelectric effect can be explained in terms of classical light waves and quantized matter states.)³⁷

This device is an excellent uv light detector and is even better as a charged particle detector. As a consequence, it had to be completely enclosed in a metal case except for an entrance slit covered by a LiF window. The response for a typical combination of window and detector is shown in figure eight. The only spectral line which will show a position and beam intensity dependence and be detected is L_{α} .

The light collection geometry is shown in figure nine, and the effect of the finite slit width is discussed in appendix B. An incident uv light pulse gives an electrical output pulse on the order of 50 mV with negative polarity. This was fed into a standard NIM scintillation preamplifier which gave it the appropriate shape for use in an NIM pulse amplifier. This then fed a scaler/timer.

Figure eight: Detector response. The transmission properties of LiF^{57} and the sensitivity of the CEM detector⁵⁸ can be combined to give the optical window of the L_{α} detector.

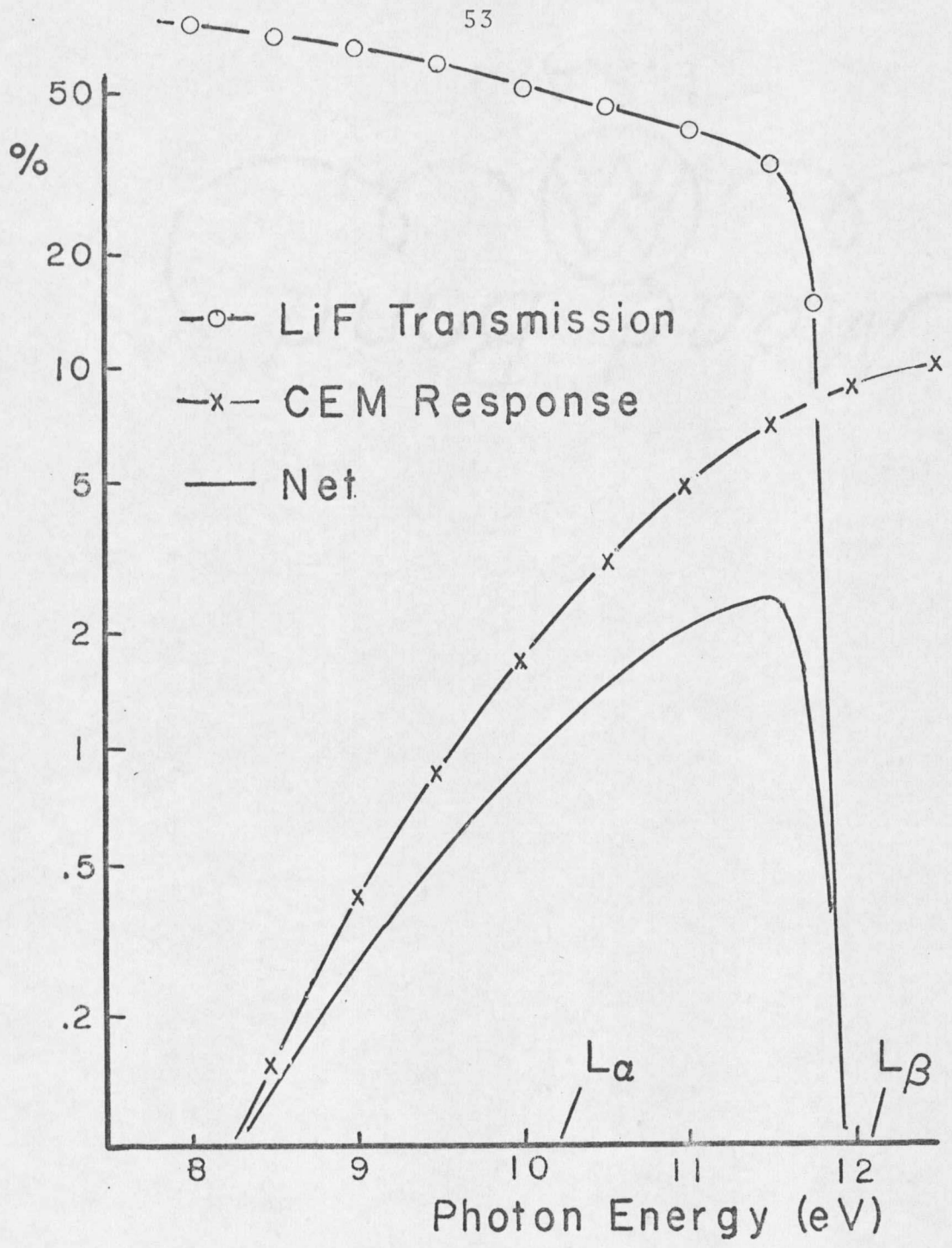
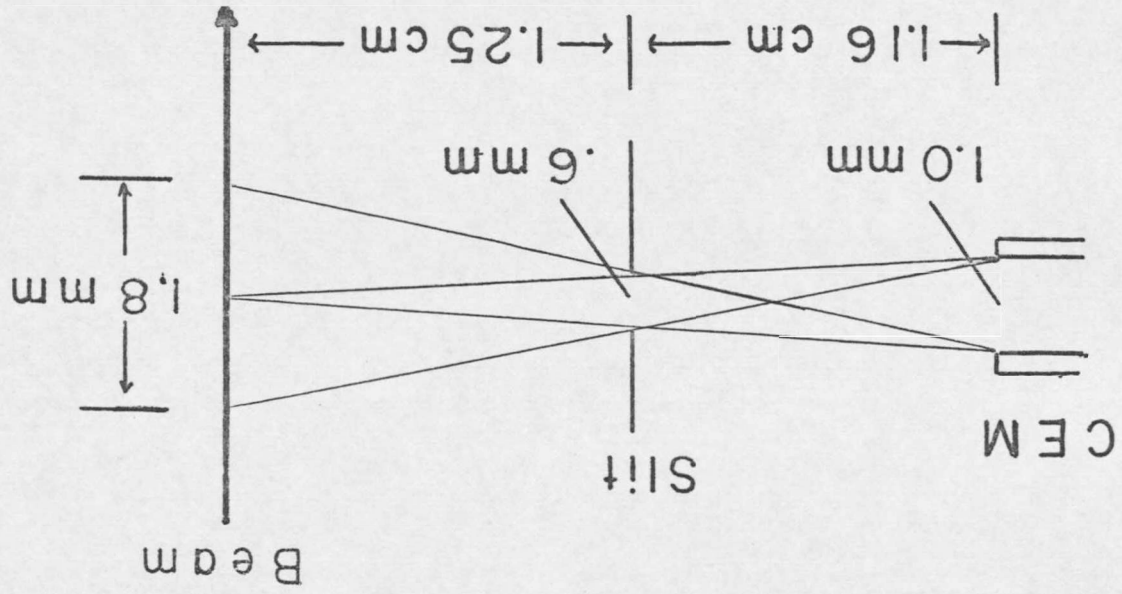


FIG 8

Figure nine: Light collection geometry. The CEM aperture was nominally 1.0 mm. The slit was 0.32 cm high and constructed of .002" shim stock pieces. The LiF window was between the slit and the detector.

FIG 9



These steps are outlined in figure ten. The electrical circuit for the channeltron is shown in figure eleven.

Light from any point along the beam could be monitored by moving the detector which was mounted on an aluminum cart that traveled on linear bushings. The cart was pushed upstream by a rod which entered the vacuum through an O-ring grease seal and returned by the pull of a weight which hung into the throat of the chamber diffusion pump. The position of the cart was set with a micrometer head at the end of the rod. With the use of spacers a total throw of five inches could be used if desired.

The neutral beam current was measured by the secondary electrons ejected from an aluminum target. The ejection efficiency for neutral atoms in the kilovolt range runs from 1.10 to 1.25 times the easily measured value for protons.⁵⁹ For a fixed energy experiment this variation is unimportant. The Faraday cage system is shown in figure twelve. It could be set to read the current to the target and suppress the electron emission or to enhance the secondary electron current. In the former setting a neutral beam appeared to be a slightly negative current. This has been observed before,⁶⁰ and

Figure ten: Electronic flow chart. The signals to be processed were a varying dc current and random negative 50 mV pulses. The recorder output of the ammeter was converted to a proportional frequency which was counted to integrate the beam charge on scaler B. Scaler A would either count a preset number of pulses while displaying the elapsed time or would count for a preset length of time.

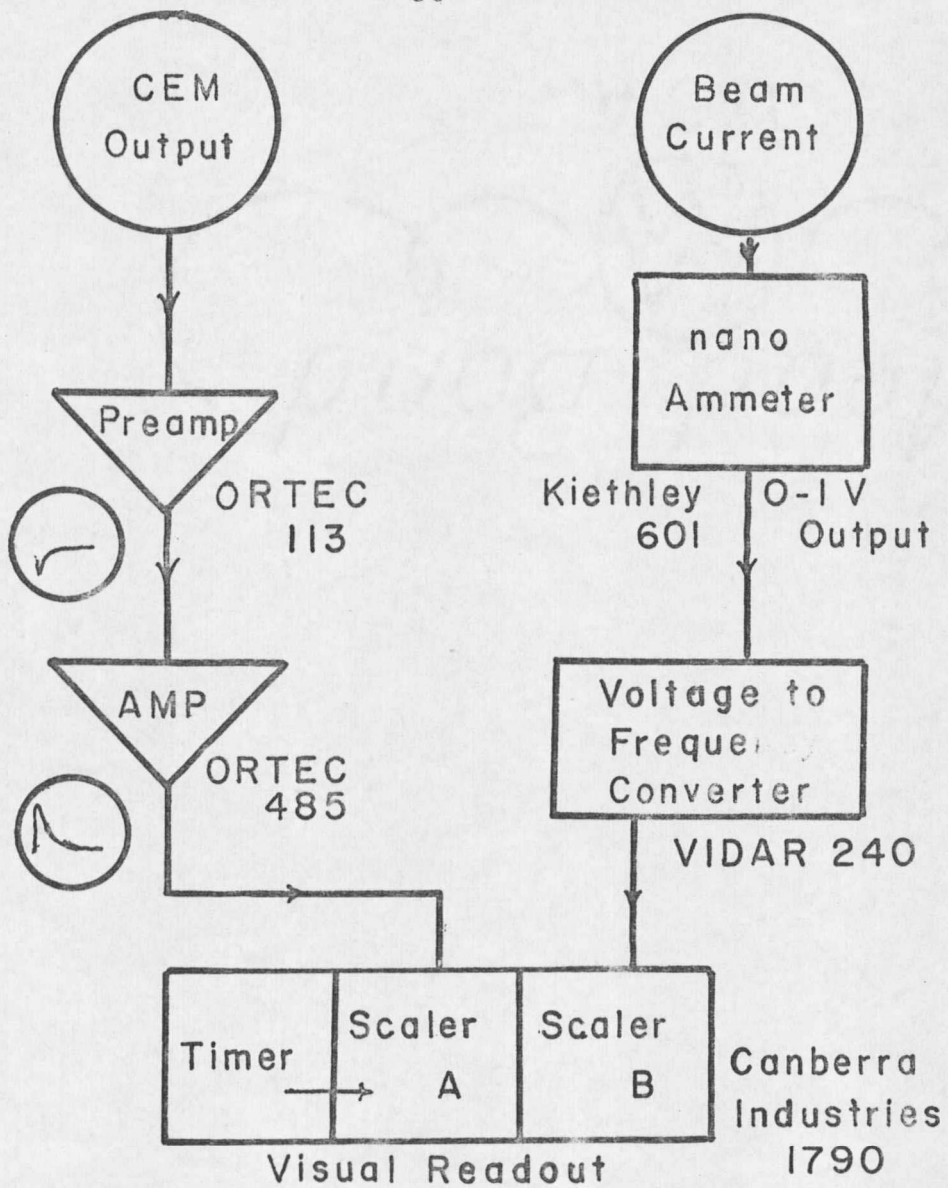


FIG 10

Figure eleven: CEM circuit. The current pulse put out by the CEM is converted to a voltage by the $1\text{ M}\Omega$ load resistor. The capacitor blocks the 2600 V potential applied to the CEM and provides a low impedance path for the pulse. The voltage divider made possible the use of two detectors during the preliminary studies.

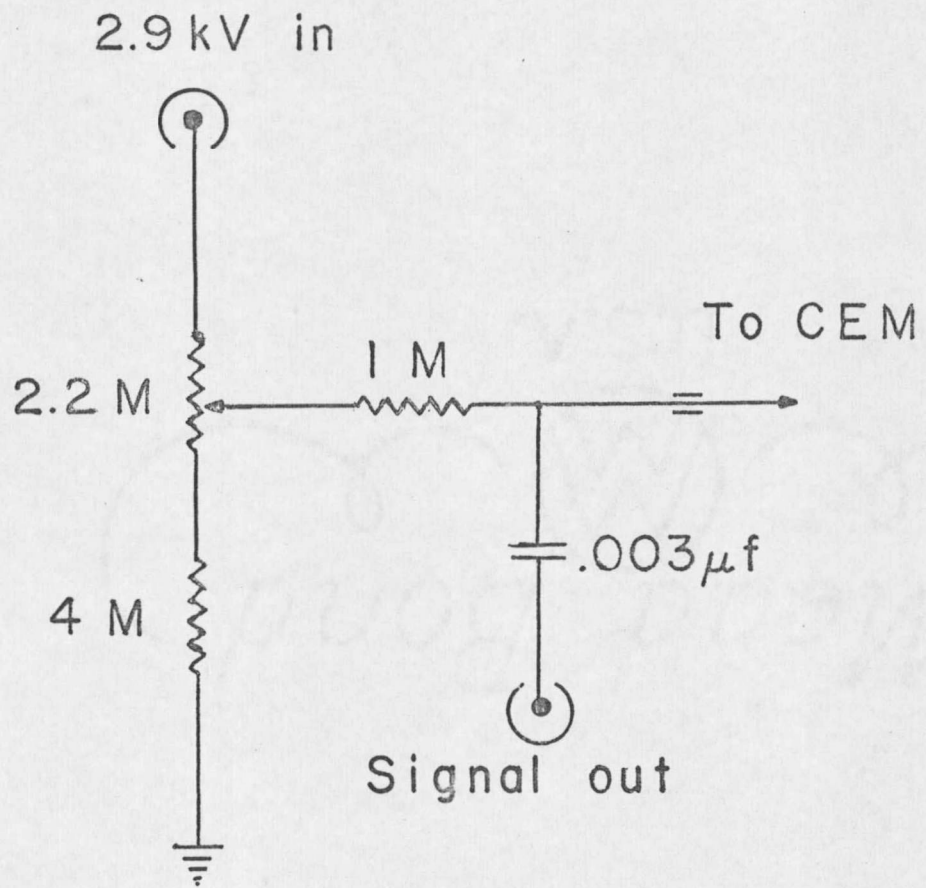


FIG II

Figure twelve: Beam detector. The neutral beam was detected by a modified Faraday cage. When the potential applied to the cup was reversed, the secondary electrons were repelled back to the target giving a true measure of the charged beam component. Only the two relevant switch positions are shown. The collection characteristics are given in figure thirteen.

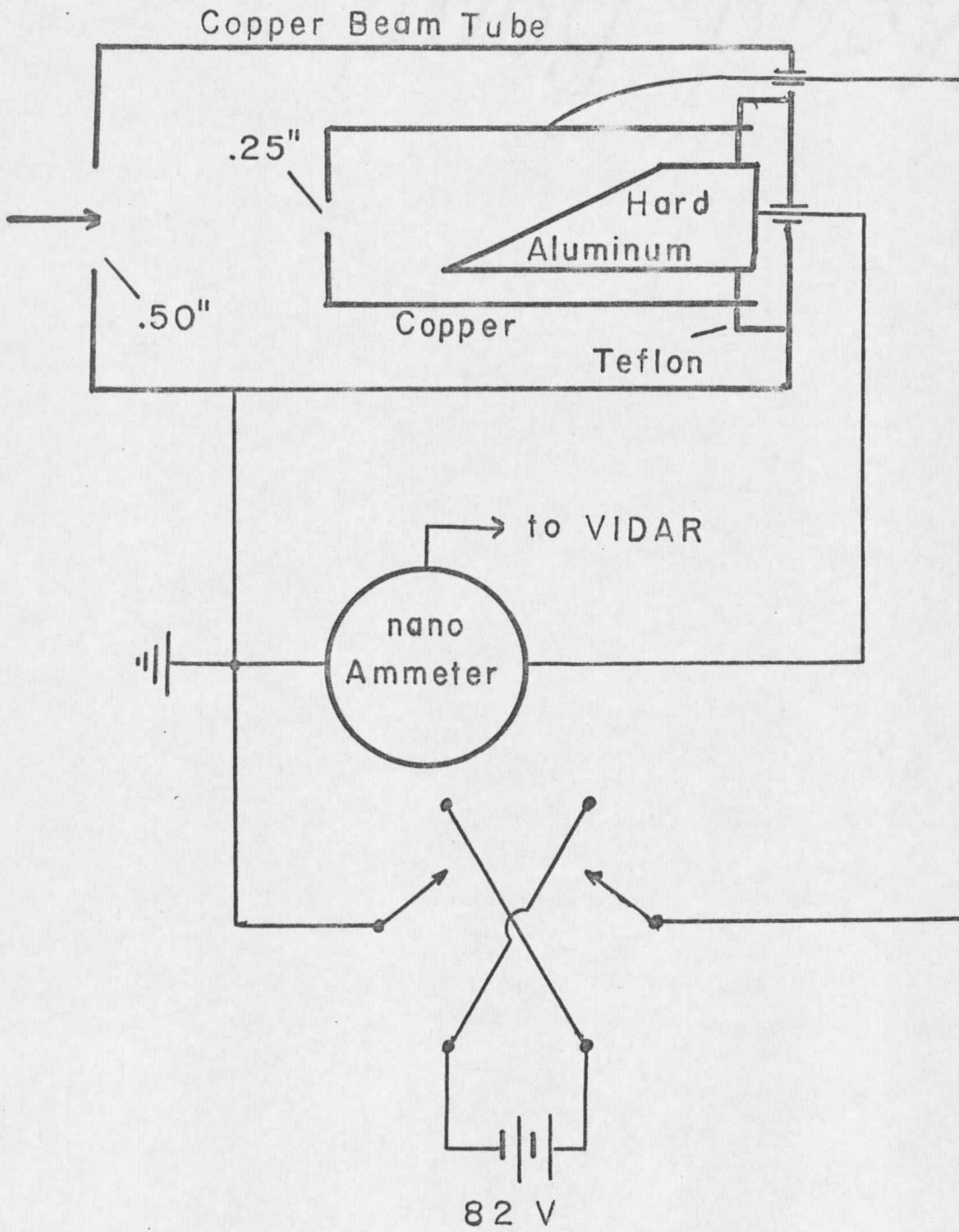


FIG 12

Figure thirteen: Collector characteristics. The current registered by the meter is shown for a fixed proton current and a variable cup potential. Note the break in the scale.

